XLVI CILAMCE
VITÓRIA - ES - BRAZIL - 2025
XLVI IBERO-LATIN AMERICAN CONGRESS ON COMPUTATIONAL METHODS IN ENGENEERING

Assessment of mesh sensitivity of hot spot methods applied to offshore structures

Gabriel C. Rodrigues[1], Carlos E. de Souza[1], Bruno Klahr [1], Daniel M. de Leon [1]

[1]*Dept. of Mechanical Engineering, Federal University of Rio Grande do Sul*
Rua Sarmento Leite, 425, Porto Alegre,90046-902, RS, Brazil
gcrmestre@gmail.com, ce.souza@ufrgs.br,00206849@ufrgs.br,daniel.leon@ufrgs.br

Abstract. To execute fatigue analysis of offshore structures, it is important to adequately determine the stresses field, especially on welds. Welded regions tend to have significant stress concentration. To deal with this problem, some international standards suggest the hot spot stress (HSS) method to estimate the stresses near welds, including guidelines for finite element analysis. Two strategies of HSS calculations are considered here: surface-extrapolated stress and through-thickness linearized stress. Recommendations exist for elements sizes of mesh depending on element type, geometry and method for HSS calculation. In this work, the calculations are applied initially to a simple flat model with different meshes, with varying element sizes and proportions between the three dimensions. Next, the strategies are applied to more complex structure, representing a bell mouth used in offshore oil platforms. Being mostly a cylindrical geometry, meshing is controlled mainly by the number of elements in thickness as well as element size in circumferential and axial direction. Different loads were applied on each case to verify mesh sensitivity relation with load type. Results indicate different levels of effect on HSS results for each direction of mesh refinement. The relation of sensitivity of the mesh with the load applied is shown and discussed.

Keywords: hot spot stress; finite element analysis; offshore structures; mesh sensitivity; complex geometry

1 Introduction

In the oil and gas industry, offshore structures are very expensive equipments that are subjected to a very harsh environment. These structures need to be designed considering failure under fatigue, due to the oscillatory loads generated by sea waves. Fatigue life becomes an important aspect in the design of such equipments, aiming longer lifespan and reliability.

To analyze fatigue, it is necessary to establish the stress field for different load cases. It is common to use computational methods like the finite element method to be able to determine stress on those cases . However, one of the limitations of the finite element method is that in many points of the structure, stress concentrations happen, and can be potentially higher than what they should be. Those points commonly happen in welded regions between parts. To deal with that problem, hot spot stress (HSS) methods were developed [1], some of them recommended in Standards for offshore structures.

Between the existing methods for computation of HSS, two are studied in this article: surface-extrapolated hot spot stress (SEHSS) and through-thickness linearized hot spot stress (TTHSS). They follow different approaches but it is expected that both can offer similar results for stress and fatigue life.

Generally, HSS methods are studied by applying them to relatively simple geometries, with simple load cases, like two welded plates in bending or tension [2]. When complex geometries and problems are involved, loads can generate stress distributions that may affect results differently for each method. A bell mouth is an example of a structure that has different types of loads applied to it throughout its life cycle. It is important to verify mesh sensitivity of the hot spot stress methods applied to the more complex geometry and if they offer adequate results under those circumstances.

An example of work studying HSS methods in more complex structures, made from many welded plates, is the work of Iqbal et al.[3], in which some methods were analyzed for a rib-to-deck joint of an orthotropic steel deck. After studying results of the methods for various meshes, in the guidelines and conclusion section the TTHSS method was considered to have performed better than the SEHSS method, especially compared to linear surface extrapolation (as quadratic extrapolation was also studied).

Previous studies comparing different meshes and loads on simple geometry were made before, like in the

work of Poutiainen[4]. In that case, similar results between SEHSS and TTHSS were obtained for different loads on a 3D model of gusset welded on a plate. In the article of Li et al. [5], three hot spot methods were compared using Finite Element Analysis, including SEHSS. Two geometries of two same thickness plates welded transversely were investigated, differentiated by the geometry of the weld. Experimental tests were made based on those geometries. A nominal stress was calculated so a stress concentration factor was obtained from hot spot results divided by that nominal stress. In that paper, the results showed that the SEHSS could significantly overestimate the stress compared to the experimental results. However, when very coarse meshes were used, the results would underestimate stress for bending load. The results show that it is important to use an adequately refined mesh.

Considering those aspects, the present work aims to study mesh sensitivity of two hot spot methods (SEHSS and TTHSS) under different loads. A reference case is studied first for a simple geometry, as a reference case to understand what would be expected for hot spot stress results. Then, the analysis of the bell mouth is applied, using a simplified bell mouth model.

In the remaining of this paper, we summarize the two HSS methods that will be evaluated. Two geometries with different level of complexity are studied and described in section 3. The results are presented and discussed in section 4, followed by general concluding remarks.

2 Hot spot stress methods

Hot spots stress methods consist in approaches to approximate stress on numerical models of weld toes. To avoid overestimation the stress on the weld margins, the hot spot approximations aim to obtain an effective stress that can be used for fatigue life computation. The DNV RP 203 standard [6] presents two methods for effective stress hot spot stress approximation: (I) section 3.1: hot spot stress from extrapolation on the surface; and (II) section 3.2: hot spot stress from linearization through the plate thickness, by combining membrane and bending stress components. In this paper, these two method are applied to two different geometries, and the resulting stress are compared. The methods are detailed below.

2.1 Hot spot stress with extrapolation to the surface

The SEHSS follows the instructions given in section 4.3.4 and 4.3.4 of DNV RP C203 [6]. In this case, the stress at the weld toe (the hot spot position) is computed by means of a linearization of stress obtained on the surface at positions $0.5t$ and $1.5t$ from the weld to, where t is the base metal plate thickness. Figure 1a shows a reference of directions and position for weld toe stress computation.

The first phase consists in computing the stress at the points on the surface, at positions $0,5t$ and $1,5t$. For each of the points, the full stress tensor is obtained in Abaqus/CAE, using the *Path* tool to interpolate all the stress components represented by $\sigma_{0,5t}$ and $\sigma_{1,5t}$. From the full tensor, the main stress on the tensor are computed.

The stress at the weld toe is computed by the following linearization:

$$\boldsymbol{\sigma}_{HS} = 1.5\boldsymbol{\sigma}_{0.5t} - 0.5\boldsymbol{\sigma}_{1.5t} \tag{1}$$

where σ_{HS} is a full stress tensor. The stress $\boldsymbol{\sigma}_{0.5t}$ and $\boldsymbol{\sigma}_{1.5t}$ are the full stress tensor obtained directly from Abaqus/CAE at the points 0.5t and 1.5t .

From σ_{HS}, the in-plane stress perpendicular ($\sigma_{\perp}$) and parallel ($\sigma_{\parallel}$) to the weld, as well as the in-plane shear stress $\tau_{\parallel}$ (See Fig 1a) are computed from the following transformations:

$$\sigma_{\perp} = \mathbf{s}^T\boldsymbol{\sigma}\mathbf{s} \qquad \sigma_{\parallel} = \mathbf{t}^T\boldsymbol{\sigma}\mathbf{t} \qquad \tau_{\parallel} = \left[\boldsymbol{\sigma}\mathbf{s} - \left(\mathbf{s}^T\boldsymbol{\sigma}\mathbf{s}\right)\mathbf{s}\right]\cdot\mathbf{t} \tag{2}$$

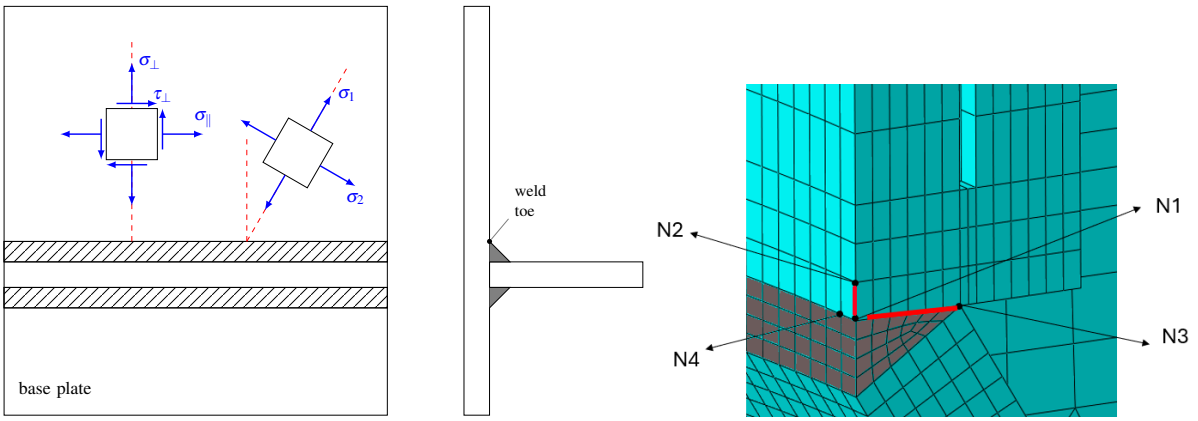
where $\mathbf{s}$ and $\mathbf{t}$ are unitary vectors that define the direction normal to the weld and parallel to the weld, respectively. To compute these vectors, the nodes N1, N2 and N4 (Fig. 1b are chosen on the FE mesh. Vector $\mathbf{s}$ is obtained form the difference $N2 - N1$, and vector $\mathbf{t}$ comes from the difference $N4 - N1$. Next, the two main stresses are computed from the in-plane components of eq.(2) :

$$\sigma_1 = \frac{\sigma_{\perp} + \sigma_{\parallel}}{2} + \frac{1}{2}\sqrt{\left(\sigma_{\perp} - \sigma_{\parallel}\right)^2 + 4\tau_{\parallel}^2} \qquad \sigma_2 = \frac{\sigma_{\perp} - \sigma_{\parallel}}{2} + \frac{1}{2}\sqrt{\left(\sigma_{\perp} - \sigma_{\parallel}\right)^2 + 4\tau_{\parallel}^2} \tag{3}$$

As per DNV RP C203 [6], the amplitude of the effective stress can be computed from those stress components:

$$\Delta\sigma_{eff} = \max\begin{cases}\sqrt{\Delta\sigma_{\perp}^2 + 0.81\Delta\sigma_{\parallel}^2}\\ \alpha\left|\Delta\sigma_1\right|\\ \alpha\left|\Delta\sigma_2\right|\end{cases} \tag{4}$$

where the value of α might be 0.72, 0.80 or 0.9, depending on the classification of the weld detail, according to Appendix A of Ref. [6].



(a) Representation of the stress components on the path perpendicular to the weld and the main stress on a certain orientation [6].

(b) Nodes necessary to define the directions for hot spot stress calculation.

Figure 1. Points and path used for computation of HSS on Model 1.

2.2 Through thickness hot spot stress linearization

The TTHSS follows the premises proposed in section 4.3.6 of DNV RP C 203 [6]. In this case, the HSS at the weld toe is computed by the combination of membrane and bending stress at that point. These stress components are obtained by means of a linearization of stress through thickness. The linearization process is performed in Abaqus/CAE interface, using the tool *Stress linearization* along a *Path* define by nodes N1 and N3 (see fig 1b).

The membrane stress represents the constant, or average, stress component through thickness. All components of the stress tensor are computed by means of the integration

$$\boldsymbol{\sigma}_m^{local} = \frac{1}{t}\int_{-t/2}^{t/2} \boldsymbol{\sigma}(s)\,\mathrm{d}s \tag{5}$$

where t is the section thickness, $\boldsymbol{\sigma}$ is the stress tensor along the *path* and s is the coordinate along the Path where the stress is probed [7, 8]. The bending stress is equivalent to a linear stress variation, which is computed considering the difference to the membrane component, such that

$$\boldsymbol{\sigma}_b^{local} = \frac{6}{t^2}\int_{-t/2}^{t/2} \left(\boldsymbol{\sigma}(s) - \boldsymbol{\sigma}_m^{local}\right) s\,\mathrm{d}s \tag{6}$$

Once the two components are computed, the reference HSS is given by the sum:

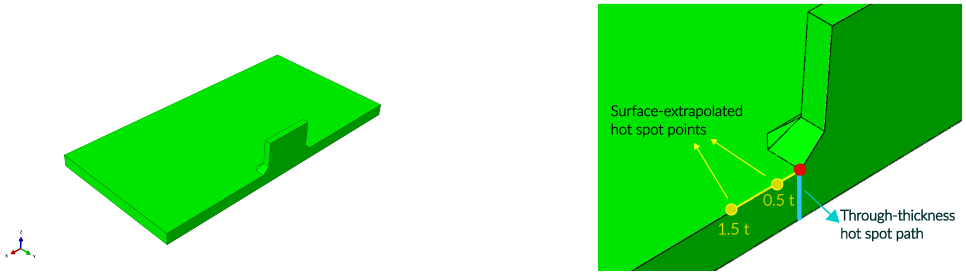
$$\sigma_{HS} = \sigma_m^N + \beta\sigma_f^N \tag{7}$$

where β is a multiplication factor for the bending stress, which usually is defined between 0.6 and 1.0.

3 Methodology

To evaluate and compare the HSS methods, they are applied to two models, i.e., a simple geometry composed of flat plates (Model 1), and a more complex model representing a component of an offshore riser, made with cylindrical, conical and flat plates (Model 2). The reference geometry (Model 1) is based on the work of Li and Choung [5], following the drawings and dimensions. The same boundary conditions of the three-point bending test were applied as presented by the article. The load was a force of 14710 N in the z direction applied to nodes at the same location of the bending test of the original article. The SEHSS method was applied using two points along the longitudinal direction (x axis), at the surface where the welding is located, in two different distances from the studied point: one point at half the plate thickness (t) and the other at 1.5 times the thickness of the plate. The TTHSS was applied using a path aligned with the thickness direction and the analyzed point. In Fig. 2 the

geometry and location of the SEHSS points and TTHSS path are shown. Three meshes were generated in this geometry to asses mesh convergence.



(a) Isometric view with longitudinal cut of two plates geometry

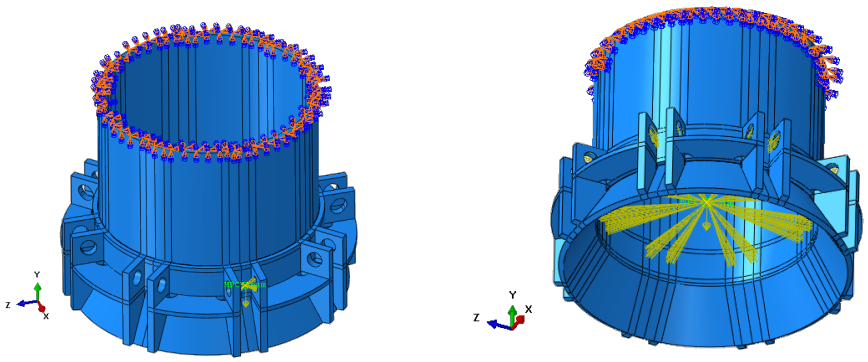
(b) Zoomed view with points and path location

Figure 2. Points and path used for computation of HSS on Model 1.

The complex geometry (Model 2) is based on a bell mouth used in risers lines of on offshore platforms. For this study, the geometry was simplified, but still remains fairly complex. In Fig. 3 the geometry is shown with boundary conditions applied. The geometry has a cylindrical region and a conical region. The point of interest for that geometry is located on the circumferential weld connecting those regions. There are also 8 pairs of vertical plates with holes welded to both those regions of the geometry. The vertical plates connect indirectly to the cylindrical region through a reinforcing ring. There are also horizontal plates connecting the vertical plates from different pairs.

Two loads of the same value and direction were applied in that case. The value of the force is 100 kN and the direction is minus y. For Load 1, the force is applied on a point aligned with the center of the holes of one pair of plates with the point connected rigidly to the holes of that one pair. As for Load 2, the force is applied on a point at the same height as Load 1, but at the center of the diameter of the simplified Bell Mouth, with the point connected to all the vertical plates' holes, generating an equally distributed force on all pairs of vertical plates.

For each main direction of the mesh around the analyzed point (thickness, circumference, and height), two element sizes were chosen. Combinations of those sizes result in 8 meshes in total. Figure 4 shows the regions affected and localization of the point analyzed with hot spot methods.



(a) Load 1

(b) Load 2

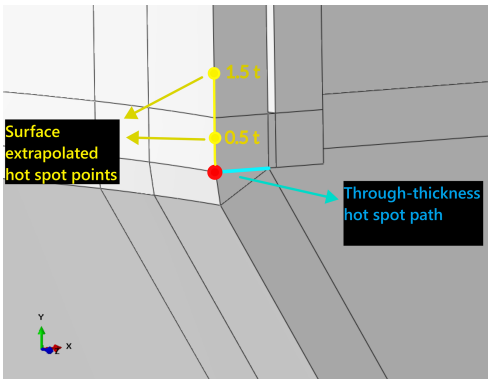
Figure 3. Boundary conditions and loads for Model 2 (simplified bell mouth).

4 Numerical studies

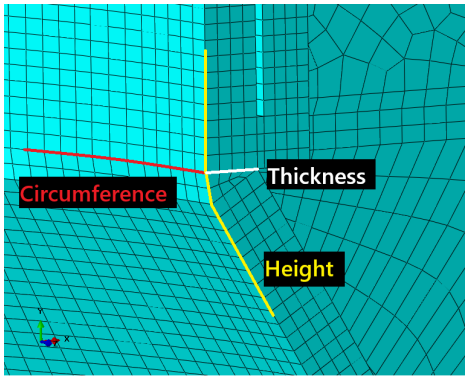
In this section, the results for both geometries are shown. First, the sensitivity to the mesh of Model 1 is presented, followed by Model 2 results and discussion. Linear hexaedric elements with reduced integration were used (C3D8R in Abaqus) in both models.

4.1 Model 1 - reference model

Results for the two-plate geometry are shown in Tab. 1. The three meshes have a maximum global size of elements of 5mm, but each mesh has a different local size specified around the weld: Mesh 1 has 5mm, Mesh 2



(a) Position of points for HSS computation



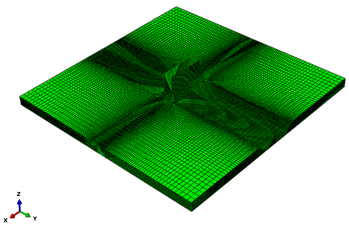
(b) Directions for mesh refinement represented over mesh 1

Figure 4. Definition of points for HSS computation and directions of mesh refinement on Model 2.

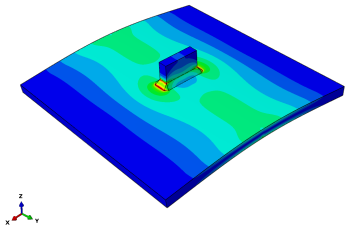
has 3mm and Mesh 3 has 1.5mm of local size. In this case, increasing mesh density increased stress results. While Mesh 3 is significantly more refined than the other two, it seems even more elements would be needed for better convergence. However, it can be observed from the three meshes that results for applying the bending in the *y* axis show significantly higher values for TTHSS compared to the SEHSS.

Table 1. Stress results for bending in y direction on Model 1.

	TTHSS			SEHSS		
	σ_m	σ_b	Resulting	σ_I	σ_{II}	Resulting
Mesh 1	4.208	55.043	59.251	57.379	20.355	57.379
Mesh 2	4.738	61.708	66.446	58.249	21.09	58.249
Mesh 3	4.839	64.084	68.923	60.558	22.489	60.558



(a) Geometry with mesh 3



(b) Stress field

Figure 5. Model 1, showing mesh 3 (a) and stress field (b) .

4.2 Model 2 - simplified bell mouth

The Model 2 is a simplified bell mouth, showing a more complex geometry than Model 1. Around the region of the studied point, many paths for load distribution exist that may change stress components results compared to the welded plate case. Table 2 and 3 show results for the bell mouth for each load case.

Results for Load 1 show a large difference between the methods. The region of interest is in a state where bending and membrane stress oppose each other, generating lower results for the TTHSS. It is difficult to determine all the effects causing that behavior. As the mesh is refined, the amplitude of bending stress component of the TTHSS method increases (larger negative values). Since it opposes the membrane stress, resultant stress decreases with mesh refinement. Differences of Mesh 1 to Mesh 2 and Mesh 5 to Mesh 6 is small, particularly for the TTHSS. The difference of Mesh 1 and Mesh 5 point to higher sensitivity to thickness, which makes sense for the TTHS method. Element size in vertical direction has an intermediary influence.

The SEHSS resultant stress is not affected as much by the mesh proportionally. The σ_I component is much bigger than σ_{II} component, so the resultant stress for that case is always σ_I. Circumference refinement actually

slightly reduces value for the SEHSS stress components. Reduction of element size in height shows slight increase in stress, while refining in thickness also increases stress, but with higher influence.

Both methods are closer with Load 2 applied, with the SEHSS having lower resultant stress. Analyzing TTHSS sensitivity for thickness refinement is more impactful on the bending component, but the membrane component is barely changed. The resultant stress for TTHSS seems very little sensitive for Load 2.

As for the SEHSS in Load 2, the element size in height has significant influence in the resultant stress. The stress components are both more sensitive towards height refinement. Mesh size changes in circumference and thickness influence the results much less.

Table 2. Stress results on simplified bell mouth for load case 1

	Mesh size (mm)			TTHSS			SEHSS		
	Thickn.	Height	Circumf.	σ_m	σ_b	Result.	σ_I	σ_{II}	Result.
Mesh 1	4.5	5	8	9.143	-6.765	2.378	11.141	6.104	11.141
Mesh 2	4.5	5	4	9.009	-6.682	2.327	10.999	6.031	10.999
Mesh 3	4.5	3	8	9.152	-7.18	1.972	11.256	6.491	11.256
Mesh 4	4.5	3	4	9.072	-7.164	1.908	11.107	6.399	11.107
Mesh 5	2.5	5	8	9.611	-8.12	1.491	11.469	5.857	11.469
Mesh 6	2.5	5	4	9.54	-8.095	1.445	11.314	5.786	11.314
Mesh 7	2.5	3	8	9.527	-8.473	1.054	11.55	6.371	11.55
Mesh 8	2.5	3	4	9.45	-8.458	0.992	11.386	6.271	11.386

Table 3. Stress results on simplified bell mouth for load case 2

	Mesh size (mm)			TTHSS			SEHSS		
	Thickn.	Height	Circumf.	σ_m	σ_b	Result.	σ_I	σ_{II}	Result.
Mesh 1	4.5	5	8	0.597	0.193	0.79	0.702	0.157	0.702
Mesh 2	4.5	5	4	0.596	0.190	0.786	0.698	0.152	0.698
Mesh 3	4.5	3	8	0.598	0.197	0.795	0.747	0.170	0.747
Mesh 4	4.5	3	4	0.596	0.192	0.788	0.742	0.165	0.742
Mesh 5	2.5	5	8	0.603	0.171	0.774	0.697	0.174	0.697
Mesh 6	2.5	5	4	0.602	0.167	0.769	0.693	0.168	0.693
Mesh 7	2.5	3	8	0.604	0.178	0.782	0.752	0.185	0.752
Mesh 8	2.5	3	4	0.603	0.172	0.775	0.746	0.179	0.746

While the results of the two loads can't be compared to each other directly, some observations can be made. Changing boundary conditions may change how the two HSS methods compare to each other. In one situation, they can be closer. In another, they can be vastly different. The mesh was changed in only two different sizes for each of the three directions, so more meshes would be needed for good understanding of effect of mesh sizes in each direction. However, some tendencies can be observed:

The TTHSS method was particularly affected by thickness and height in Load 1, but very little effect from circumference refinement. The SEHSS method showed small changes in Load 1 caused by refinement in thickness (around .3 MPa of difference, less than 3% difference), while circumferential and height refinement changes are smaller in intensity, but circumferential refinement decreases stress while height refinement increases it.

In Load 2 the TTHSS method was only significantly affected by mesh size in thickness, but that was still a small influence (around .15 MPa difference). As for the SEHSS, it was only significantly by refinement in height. The 3mm height led to larger resulting stress values (approximately .75 MPa) compared to the 5 mm cases (around .70 MPa).

Overall, circumference was the least influential direction for mesh size in all cases. Height and thickness both affected results significantly, depending on the case. Results indicate different mesh sensitivities for each HSS method and for each load.

The same value of force was applied on the same direction, but on different regions and from a different

point. The stress state at the region of interest tends to change with the different boundary conditions. Considering the geometry features around the point studied, a simple vertical force applied at only one pair of plates can generate a complex distribution of loads in those conditions. The TTHSS method considers membrane and bending components normal to the path, but other effects could be actuating in this case that SEHSS method captures. Applying the same force on all the pairs, the two methods become more similar. There is less bending component on TTHSS method. Load 2 makes the problem more symmetrical, as the 8 circumferential slices are in the same condition. That has implications on how stress state is around the analyzed point.

5 Conclusions

In this work a study of two HSS methods was applied in a reference geometry (Model 1) and then a investigation was made with different mesh sizes in a complex geometry (Model 2). For Model 1, it is observed that the mesh refinement indicates stress convergence, but it was not yet achieved with the proposed meshes. In addition, the THSSS consistently leads larger stress values that SEHSS.

For Model 2, the HSS methods were applied in two load cases, and considering a combination of two levels of refinement for each direction around the region of interest. Different sensitivities were shown for each load case. For Load 1, the TTHSS was particularly sensitive to size of elements in height and thickness. The SEHSS was not as sensitive and presented similar changes for all directions of mesh refinement, with slightly more influence of thickness. For Load 2, the sensitivity was low in both methods, except for the SEHSS method being particularly impacted by the size in height. The sensitivity to the mesh size changed based on how the load was applied. Also, the two methods presented different sensitivities compared to each other in both cases.

It is observed that caution is needed when more complex cases are studied. For Load 1 the values for the two methods are vastly different. Load 1 tends to generate a more complex stress condition around the analyzed point, while Load 2 tends to be closer to a tension, though there are still effects of interaction between the different components (plates, cylinder and skirt).

That difference of results presents a challenge, as many types of load can be applied to a bell mouth through its life cycle. Different load conditions would change which of the two methods would give the higher stress range for fatigue analysis. The difference could be very high as demonstrated by Load 1 on the simplified bell mouth.

Following this work, future investigations should be made to study mesh sensitivity of HSS methods under other boundary conditions, and should analyze how different methods compare to each other. Also, alternative methods should be investigated for the bell mouth structure, as they could prove more reliable and consistent under different load conditions.

Acknowledgements. The authors acknowledge the support from Petrobras through the cooperation term number 2022/00242-3 (UFRGS/GMAp).

Authorship statement. The authors hereby confirm that they are the sole liable persons responsible for the authorship of this work, and that all material that has been herein included as part of the present paper is either the property (and authorship) of the authors, or has the permission of the owners to be included here.

References

[1] A. Hobbacher. The new IIW recommendations for fatigue assessment of welded joints and components – a comprehensive code recently updated. *International Journal of Fatigue*, vol. 31, n. 1, pp. 50–58, 2009.

[2] J.-M. Lee, J.-K. Seo, M.-H. Kim, S.-B. Shin, M.-S. Han, J.-S. Park, and M. Mahendran. Comparison of hot spot stress evaluation methods for welded structures. *International Journal of Naval Architecture and Ocean Engineering*, vol. 2, n. 4, pp. 200–210, 2010.

[3] N. Iqbal, H. Fang, A. Naseem, M. Kashif, and H. De Backer. A numerical evaluation of structural hot-spot stress methods in rib-to-deck joint of orthotropic steel deck. *Applied Sciences*, vol. 10, n. 19, pp. 6924, 2020.

[4] I. Poutiainen, P. Tanskanen, and G. Marquis. Finite element methods for structural hot spot stress determination—a comparison of procedures. *International Journal of Fatigue*, vol. 26, n. 11, pp. 1147–1157, 2004.

[5] C. B. Li and J. Choung. A new method of predicting hotspot stresses for longitudinal attachments with reduced element sensitivities. *International Journal of Naval Architecture and Ocean Engineering*, vol. 13, pp. 379–395, 2021.

[6] D.-R.-C. Det Norske Veritas. Fatigue design of offshore steel structures, 2019.

[7] D. S. Simulia Corp. *ABAQUS/Standard User's Manual, Version 2023*. Dassault Systèmes, 2023.

[8] A. Hobbacher. Recommendations for fatigue design of welded joints and components. Technical Report IIW document XIII-2151-07. XV-1254r4-07, International Institute of Welding, 2008.